RSC Pharmaceutics

Accepted Manuscript

This article can be cited before page numbers have been issued, to do this please use: J. Pires, L. R. De Souza, B. B. Fontanezi, S. Mendanha and E. Lima, *RSC Pharm.*, 2026, DOI: 10.1039/D6PM00126B.

View Article Online
DOI: 10.1039/D6PM00126B

ARTICLE

Lipid Phase Organization Controls Drug Partitioning and Release Across Lipid Nanocarriers

Received 00th January 20xx,
Accepted 00th January 20xx

DOI: 10.1039/x0xx00000x

Jader Pires,[#a,b] Lucas R. de Souza,[#a,c] Bianca B. Fontanezi,[a,b] Sebastião A. Mendanha[a,c] and Eliana M. Lima*[a,b]

Understanding how lipid organization is associated with drug incorporation and release across nanocarrier platforms remains a central challenge in the rational design of lipid-based delivery systems. Here, lipid nanoparticles (LNP), liposomes, solid lipid nanoparticles (SLN), and nanostructured lipid carriers (NLC) were systematically compared to investigate correlations between lipid composition, local structural order, and release behavior. Dexamethasone was employed as a model lipophilic probe to investigate molecular partitioning across these distinct lipid environments. Nanocarriers were characterized in terms of size, polydispersity, zeta potential, encapsulation efficiency (EE), and drug loading (DL), while lipid dynamics were resolved by spin-label electron spin resonance (ESR) using depth-sensitive probes. In vitro release profiles were obtained at 4 and 37 °C to evaluate temperature-dependent permeability. SPC-based liposomes exhibited the highest incorporation (EE ≈ 90%; DL ≈ 45 µmol/mol) and the lowest motional restriction, as indicated by reduced rotational correlation times and $2A_{||}$ values, and displayed the slowest release kinetics. In contrast, HSPC-based liposomes generated the most ordered lipid environments, with the highest ESR-derived motional parameters, exceeding those observed for SLN and LNP, and showed rapid release at 37 °C but strong retention at 4 °C, indicating pronounced thermal sensitivity. SLN, NLC, and LNP exhibited lower incorporation (EE < 35%) and intermediate motional restriction, converging toward less favorable environments for drug accommodation despite their distinct supramolecular structures. Across all systems, encapsulation and release behavior correlated consistently with ESR-derived descriptors of lipid mobility and order rather than with nanocarrier class. These findings demonstrate that lipid phase organization, defined by composition, packing density, and dynamic heterogeneity, consistently underlies molecular accommodation and diffusion across structurally distinct nanocarriers. The ESR-derived mobility parameters reported here correlate with encapsulation efficiency and release kinetics, supporting their use as descriptors for interpreting formulation-dependent differences in drug behavior beyond conventional structural classification. Extrapolation to other hydrophobic molecules, however, may require appropriate optimization, as drug-specific membrane interactions may modulate these relationships.

Introduction

Lipid-based nanocarriers are widely used as drug delivery platforms because they allow modulation of molecular incorporation, colloidal stability, and release behavior.[1] However, predicting the behavior of a lipophilic small molecule across different lipid systems remains difficult. Although liposomes, solid lipid nanoparticles (SLN), nanostructured lipid carriers (NLC), and lipid nanoparticles (LNP) are commonly grouped as lipid-based carriers, they differ markedly in internal organization and therefore in the physicochemical environments they provide for molecular accommodation and diffusion.[1,2]

These differences are not merely nominal. Liposomes are classical bilayer vesicles,[3,4] whereas SLN are based on solid lipid matrices and NLC, formed by incorporating liquid lipids into the matrix to reduce the high crystallinity of SLN.[5,6] LNP, in turn, are more structurally complex assemblies whose internal organization differs from that of conventional bilayer vesicles.[7,8] As a result, the same molecule may experience markedly different local constraints depending on whether it partitions into a fluid phospholipid bilayer, a more ordered or partially crystalline lipid matrix, or a compartmentalized lipid assembly.[9,10]

Across these systems, key factors expected to modulate drug behaviour include the physical properties of the lipid phase itself. Lipid saturation, sterol content, lipid packing density, and structural heterogeneity may alter local mobility and permeability, thereby affecting how readily a lipophilic compound can be accommodated, retained, and released.[2] In bilayer systems, cholesterol and saturated chains generally increase local order and condense the membrane, whereas unsaturated chains tend to favor greater fluidity and packing defects.[11,12] From this perspective, carrier identity alone may be a poor predictor of molecular behavior if different formulations converge toward similar lipid-phase properties.[1,2,9]

[a.] *FarmaTec - Laboratory for RD&I in Pharmaceutical Nanotechnology and Drug Delivery Systems, Samambaia Technology Park, UFG, Goiânia – GO, Brazil*
[b.] *School of Pharmacy, Federal University of Goiás, Goiania, 74690-631, Brazil*
[c.] *Institute of Physics, Federal University of Goias, Goiania, 74605-220, Brazil*
[#] J.P. and L.R.S contributed equally to this work.
* Corresponding author: emlima@ufg.br

Dexamethasone combines physicochemical properties that are particularly suited for association with lipid nanocarriers and has been extensively employed as a model compound in lipid-based delivery systems. Dexamethasone exhibits moderate lipophilicity, with reported logP values around 1.8–1.9, and low aqueous solubility (≈89 mg/L at 25 °C), characteristics that support its incorporation into lipid nanocarriers.[13] Furthermore, dexamethasone remains predominantly non-ionized at physiological pH because corticosteroids generally possess high pKa values (>12), resulting in negligible ionization within the biological pH range.[14] Consequently, dexamethasone remains essentially neutral under physiological conditions, favoring partitioning into lipid bilayers and hydrophobic interactions with membrane phospholipids. Steroid compounds, including dexamethasone, are known to interact with phospholipid membranes and modulate bilayer organization, packing, and membrane dynamics.[15] In particular, dexamethasone has been shown to spontaneously insert into DMPC membranes and alter membrane compressibility and phase behavior.[16] Furthermore, dexamethasone is among the most extensively investigated corticosteroids in lipid-based drug delivery systems, making it a useful model compound for comparing molecular behavior across distinct nanocarrier platforms.[15,17–19]

Although studies of individual nanocarrier classes are abundant, direct comparisons that connect lipid composition, internal organization, and local dynamics to the behavior of the same lipophilic molecule remain scarce. This is particularly relevant because formulations with very different architectures may generate similar functional outcomes, whereas systems within the same nominal class may behave differently if their local lipid organization is not equivalent.[1,20,21]

Electron spin resonance (ESR) with spin labeling provides a useful means of probing these differences by resolving local order and mobility within the lipid phase.[22–24] Combined with physicochemical characterization and release measurements, this approach allows direct comparison between particle organization and the dynamic properties of the lipid environment.

In this study, dexamethasone was used as a model lipophilic probe to examine how differences in lipid composition, local order, and membrane dynamics correlate with molecular partitioning, incorporation, and release across liposomes composed of saturated or unsaturated phospholipids, SLN, NLC, and LNP. Dexamethasone represents a suitable model for investigating how lipid organization affects drug behavior because its neutral steroidal scaffold, moderate lipophilicity, and limited aqueous solubility favor membrane partitioning, properties shared by many small molecules formulated in lipid-based nanocarriers. This approach allows the relative contributions of carrier class and local lipid-phase organization to be evaluated, while recognizing that the conclusions are inherently constrained by the physicochemical properties of dexamethasone and the specific formulations investigated.

Results and discussion

Biophysical characterization

The formulations were designed to maximize comparability among the different nanocarrier classes while preserving the compositional and structural requirements necessary for the formation of each platform. Identical lipid compositions cannot be used across lipid nanoparticles (LNP), liposomes (LIP), solid lipid nanoparticles (SLN), and nanostructured lipid carrier (NLC), since each nanocarrier type requires specific components to ensure its characteristic supramolecular organization,[6,7] the selected formulations were chosen to maintain comparable lipid environments for dexamethasone incorporation. LNP were prepared using distearoylphosphatidylcholine (DSPC) as a structural lipid, with addition of 1,2-dioleoyl-3-trimethylammonium-propane (DOTAP), cholesterol (CHOL), and a polyanionic molecule (PAM), which are necessary for the formation of the characteristic architecture of this carrier class. In this formulation, DSPC provides a fully saturated phosphatidylcholine framework composed of two stearoyl (C18:0) chains. Liposomes were prepared using highly unsaturated soybean phosphatidylcholine (SPC) or hydrogenated soybean phosphatidylcholine (HSPC) as the main membrane-forming phospholipids, enabling comparison between a more fluid bilayer system, associated with the predominance of unsaturated acyl chains in SPC, and a more ordered bilayer system, associated with the higher proportion of saturated acyl chains in HSPC. Because both materials are soybean-derived phosphatidylcholine mixtures, they contain a distribution of acyl-chain species rather than a single defined molecular composition, including fractions with C18 chains, but differing markedly in the balance between saturated and unsaturated components. SLN were prepared using stearic acid as the main lipid core component together with SPC and sodium taurodeoxycholate (TDC), generating a solid and more ordered hydrophobic matrix. In this context, stearic acid, a saturated C18:0 fatty acid, is directly related to the stearoyl acyl-chain motif of DSPC and is also chemically analogous, in terms of hydrocarbon saturation, to the saturated acyl-chain fractions enriched in HSPC. NLC were prepared similarly, but with partial replacement of stearic acid by oleic acid, a C18:1 monounsaturated fatty acid that reduces matrix packing and crystallinity relative to SLN;[6] this also establishes a compositional parallel with SPC, which contains unsaturated acyl-chain fractions, including C18:1-containing species, that contribute to higher bilayer fluidity. Thus, although each nanocarrier class was formulated according to its own structural requirements, all systems retained a common comparative basis defined by related lipid building blocks, hydrophobic drug partitioning, and controlled differences in saturation, sterol incorporation, lipid packing, and architectural organization.

View Article Online
DOI: 10.1039/D6PM00126B

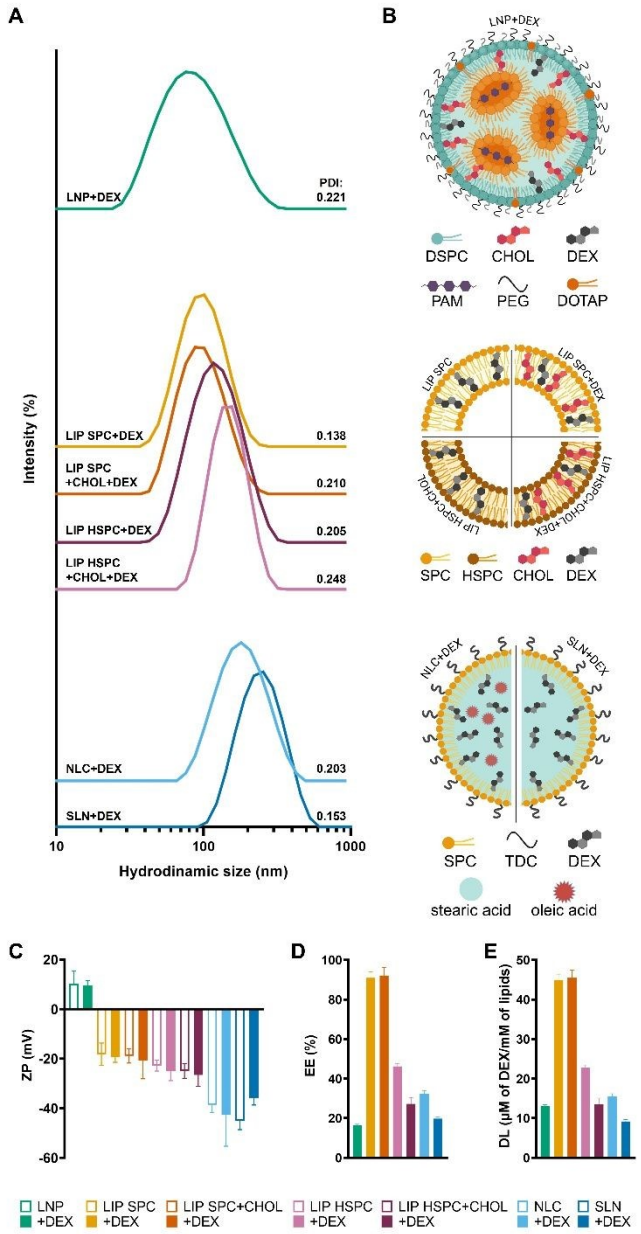

Figure 1 - Schematic representation and physicochemical parameters of lipid nanoparticles. (A) Dynamic light scattering size distribution with polidispersity index. (B) Schematic representation of lipid nanoparticle (LNP) composed of distearoylphosphatidylcholine (DSPC), cholesterol (CHOL), dexamethasone (DEX), polyanionic molecule (PAM), DSPE-PEG2000 and DOTAP; liposomes (LIP) composed of SPC or HSPC, CHOL and DEX; nanostructured lipid carrier (NLC) composed of SPC, taurodeoxycholate (TDC), DEX, stearic acid and oleic acid; and solid lipid nanoparticle (SLN) composed of SPC, TDC, DEX and stearic acid. (C) Zeta potential (ZP, mV). (D) Encapsulation efficiency (EE, %). (E) drug loading (DL, µmol of DEX per mol of lipids). Data for C, D and E expressed as mean ± SD (n = 3).

The physicochemical properties of the lipid nanocarriers are summarized in Figure 1 and Table S1 (Supplementary Material). LNP formulations exhibited mean hydrodynamic diameters of approximately 80 nm. Liposomal formulations ranged from about 100 to 160 nm, whereas SLN and NLC displayed mean sizes close to 200 nm. All formulations presented polydispersity index (PdI) values between 0.1 and 0.3, consistent with relatively narrow size distributions. Zeta potential measurements further differentiated the systems in terms of interfacial electrokinetic behavior. LNP exhibited slightly positive zeta potential values, whereas liposomal formulations showed negative values around −20 mV. SLN and NLC presented more negative zeta potentials, around −40 mV, consistent with the contribution of TDC to the interfacial potential of these systems.[6] Nanoparticle tracking analysis indicated particle concentrations on the order of 10^{13} particles/mL for all formulations.

The largest differences among formulations were observed for encapsulation efficiency (EE) and drug loading (DL). SPC-based liposomes showed the highest dexamethasone incorporation, with EE values close to 90% and DL values around 45 µmol of dexamethasone per mol of lipids. HSPC-based liposomes showed substantially lower incorporation, with EE values of 46% and 27% and corresponding DL values of 22 and 13 µmol/mol, respectively. SLN and NLC also exhibited limited dexamethasone incorporation, with EE values of 32% and 19% and DL values of 15 and 9 µmol/mol, respectively. LNP showed the lowest incorporation, with EE below 20% and DL around 13 µmol/mol.

These results indicate that dexamethasone accommodation depends on the local physicochemical properties of the lipid phase, including interfacial organization, lipid packing, and chain order, rather than simply on the presence of a hydrophobic domain.[9,10,25,26] In this context, the higher incorporation observed in SPC-based liposomes is consistent with a less ordered and more fluid bilayer environment, which may provide a more favorable setting for dexamethasone partitioning and accommodation. In contrast, the reduced dexamethasone loading in HSPC-based liposomes is consistent with a more ordered membrane environment, in which increased acyl-chain order and tighter lipid packing reduce the availability of favorable sites for drug accommodation. CHOL further decreased incorporation, consistent with its condensing effect on phospholipid bilayers and the associated increase in lipid order.[11,15]

A similar interpretation applies to SLN and NLC. Their lower incorporation is consistent with lipid environments of reduced structural flexibility and lower solubilization capacity. Although oleic acid in NLC is expected to reduce matrix order relative to SLN, this modification was insufficient under the present conditions, as assessed by ESR-derived local mobility parameters, to produce a local dynamic environment or dexamethasone accommodation profile distinguishable from that of SLN. The extent of this structural difference was not directly characterized in the present study. LNP showed the lowest EE and DL, indicating that their internal lipid organization is intrinsically less favorable for incorporation of a lipophilic corticosteroid than fluid bilayer systems.[7,27] Thus, dexamethasone loading was consistently associated with differences in local order, packing density, and accessibility of the lipid phase.

Electron spin resonance investigation of lipid dynamics

The differences in EE and DL indicate that dexamethasone accommodation depends on the motional properties of the lipid phase. To probe these features at the molecular level, lipid dynamics were investigated by spin-label ESR. ESR analysis was performed after incorporation of nitroxide spin labels, as these nanocarriers do not contain intrinsically stable unpaired electrons. The probes act as local reporters of mobility and order within distinct regions of the lipid phase.[28]

In this study, the spin labels 5-doxyl stearic acid (5d), 16-doxyl stearic acid (16d), 5-doxyl stearic acid methyl ester (5m), and 16-doxyl stearic acid methyl ester (16m) were used (Figure 2A). These probes differ primarily in the position of the nitroxide moiety along the stearic-acid-derived chain and, secondarily, in the terminal group, namely a free carboxylic acid or a methyl ester. Labels bearing the nitroxide moiety near carbon 5 probe more superficial regions of the lipid phase, whereas those bearing the nitroxide group near carbon 16 report on deeper hydrophobic regions.[28,29] Together, they resolve mobility at different depths of the nanocarriers.

Representative ESR spectra obtained with 5d and 16d are shown in Figure 2B-C, whereas representative spectra obtained with 5m and 16m are presented in Figure S1 of the Supplementary Material. The quantitative ESR parameters are summarized in Table 1. Spectral fitting yielded the rotational correlation time (τ_c), which reflects rotational mobility in the local environment. Lower τ_c values indicate faster motion, whereas higher values indicate greater motional restriction. Similarly, higher $2A_{||}$ values are associated with lower local mobility and greater order.

SPC-based liposomes exhibited the lowest τ_c values among the phospholipid bilayer systems. This result is consistent with the higher fluidity expected from their unsaturated acyl-chain composition and agrees with their higher EE and DL. The $2A_{||}$ values obtained for 5d were likewise lowest in SPC-based liposomes, ranging from 44.4 to 50.4 G, consistent with a less ordered interfacial environment.

HSPC-based liposomes, in contrast, displayed the highest τ_c and $2A_{||}$ values in the dataset. Their $2A_{||}$ values remained between 58.2 and 59.3 G, whereas LNP, SLN, and NLC remained within a lower range, near 48-52 G. Likewise, 5d-τ_c values reached 10.2-11.5 ns in HSPC-containing liposomes, well above the values observed for SLN, NLC, and LNP. The most motionally restricted local environments were therefore generated not by SLN or LNP, but by saturated phosphatidylcholine bilayers, particularly in the presence of cholesterol. This result is not immediately predicted from the nominal structural classification of the carriers. Because SLN are based on a solid lipid matrix and LNP are non-bilayer assemblies with complex internal organization,[6,7,30] both systems could reasonably be expected to impose stronger motional constraints than a liposomal bilayer. However, the ESR data indicate that HSPC-based liposomes generated the highest local motional restriction in the dataset. These results show that the ordering imposed by a saturated phosphatidylcholine bilayer, further enhanced by cholesterol, can exceed that of nominally solid or structurally complex lipid carriers at the local scale sensed by the spin probes. The relevant factor is therefore not the carrier label itself, but the molecular organization of the lipid region probed by ESR.

The depth-dependent information provided by 16d supports the same interpretation, while extending it to the inner hydrophobic region of the lipid phase. HSPC-based liposomes again showed the highest τ_c values, ranging from 3.34 to 4.17 ns, whereas SPC-based liposomes remained between 0.53 and 1.40 ns, and LNP, SLN, and NLC occupied an intermediate range of 0.92-1.84, 0.92-1.03, and 1.00-1.20 ns, respectively. Thus, the

Samples	5d	16d	5m	16m
	$2A_{||}$	τ_c	τ_c	τ_c	τ_c
LNP	50.8 ± 0.1	7.00 ± 0.10	1.53 ± 0.01	3.64 ± 0.03	0.90 ± 0.04
LNP+DEX	51.9 ± 0.2	7.50 ± 0.08	1.84 ± 0.01	4.07 ± 0.05	1.30 ± 0.05
LIP SPC	44.4 ± 0.2	4.23 ± 0.07	0.53 ± 0.04	2.09 ± 0.04	0.58 ± 0.03
LIP SPC+CHOL	47.4 ± 0.3	5.20 ± 0.25	0.80 ± 0.01	2.59 ± 0.02	0.64 ± 0.03
LIP SPC+DEX	45.6 ± 0.2	4.80 ± 0.09	0.71 ± 0.02	2.74 ± 0.04	0.56 ± 0.03
LIP SPC+CHOL+DEX	50.4 ± 0.4	7.10 ± 0.17	1.40 ± 0.02	3.09 ± 0.09	0.95 ± 0.01
LIP HSPC	58.2 ± 0.7	10.20 ± 0.55	3.34 ± 0.07	9.47 ± 0.45	3.81 ± 0.06
LIP HPSC+CHOL	59.2 ± 0.2	11.34 ± 0.45	3.99 ± 0.02	10.60 ± 1.16	3.98 ± 0.04
LIP HSPC+DEX	58.6 ± 0.1	10.70 ± 0.40	4.10 ± 0.08	9.56 ± 0.37	3.43 ± 0.02
LIP HSPC+CHOL+DEX	59.3 ± 0.2	11.50 ± 1.23	4.17 ± 0.07	10.40 ± 0.15	4.03 ± 0.04
SLN	48.4 ± 0.4	6.20 ± 0.17	0.92 ± 0.01	2.30 ± 0.10	0.61 ± 0.01
SLN+DEX	49.8 ± 0.1	6.90 ± 0.33	1.03 ± 0.02	2.86 ± 0.05	0.79 ± 0.24
NLC	48.7 ± 0.2	6.28 ± 0.08	1.00 ± 0.12	2.57 ± 0.11	0.62 ± 0.20
NLC+DEX	50.0 ± 0.1	6.97 ± 0.39	1.20 ± 0.01	2.98 ± 0.10	0.87 ± 0.01

Table 1: ESR-derived motional parameters of the formulations. Values of 2A|| were obtained from the 5d spectra, whereas rotational correlation times (τ_c) were calculated from the best fits of the 5d, 16d, 5m, and 16m spectra.

View Article Online
DOI: 10.1039/D6PM00126B

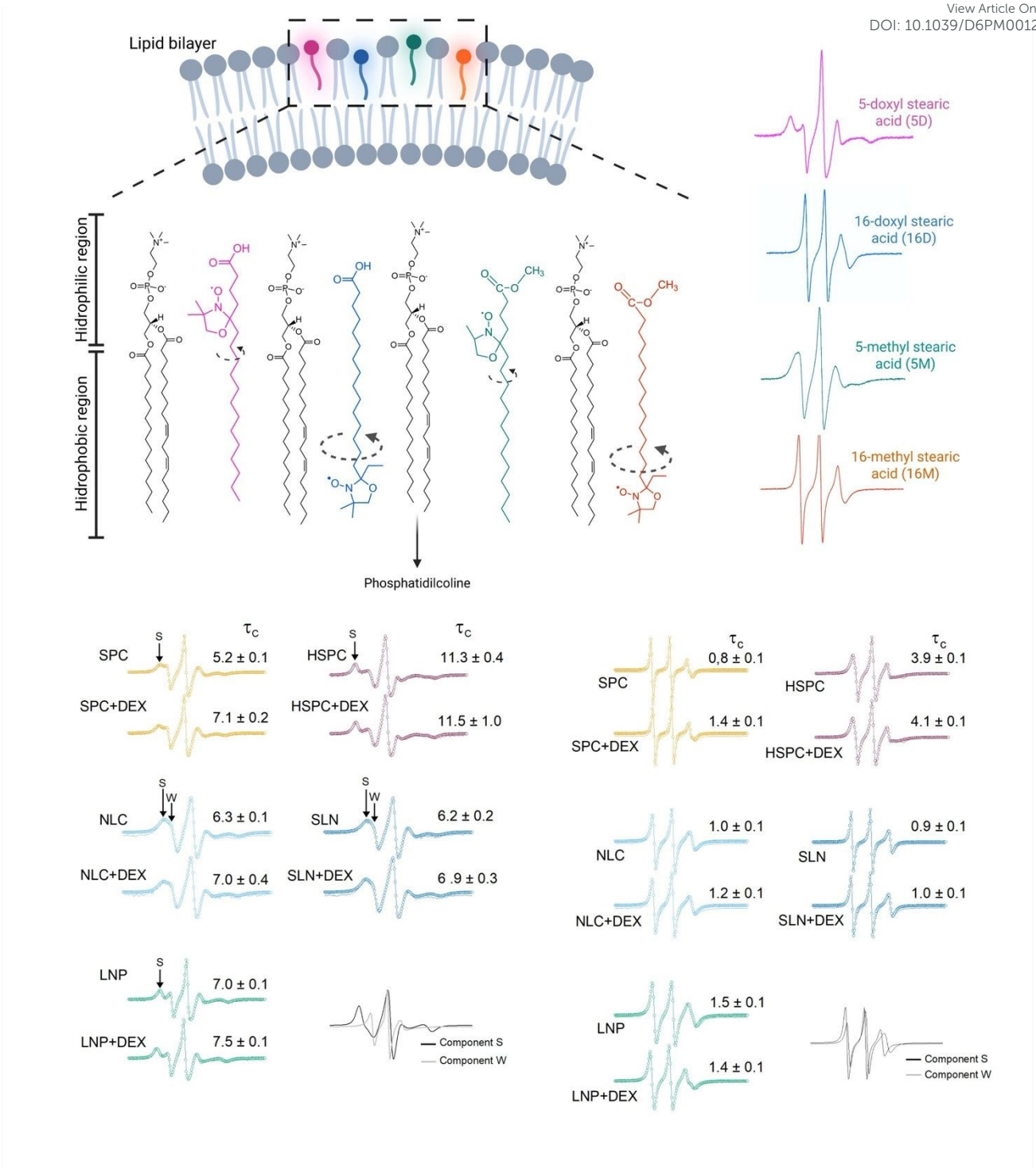

Figure 2 - (A) Schematic representation of the localization of spin labels 5D, 16D, 5M, and 16M within the lipid bilayer. The labels are incorporated at different depths, highlighting the hydrophobic and hydrophilic regions of the system. (B) Electron Spin Resonance (ESR) spectra of the 5D spin label and (C) ESR spectra of the 16D spin label for the different samples, all containing 30% cholesterol. Experimental spectra are represented by solid black lines, while open circles indicate the best computational fit used to estimate the rotational correlation time (τc). The high-mobility component (W) and low-mobility component (S) are marked with arrows in each set of spectra.

higher motional restriction observed for HSPC-containing liposomes was not limited to the more superficial region sensed by 5d, but was also maintained deeper in the lipid phase. This depth dependence is important because it indicates that the greater ordering associated with HSPC-rich bilayers extends across the membrane interior rather than being confined to the interfacial region. At the same time, the smaller numerical spread of 16d-τ_c relative to 5d-τ_c suggests that differences among formulations become less pronounced toward the bilayer center, where all systems retain greater rotational

freedom than near the interface. Even so, the persistence of the same ranking with 16d confirms that the highly ordered character of HSPC-based liposomes is a global feature of the lipid phase and not a superficial effect restricted to the headgroup-proximal region.

These ESR results also clarify the encapsulation data. The similarly low EE and DL values observed for SLN, NLC, LNP, and HSPC+CHOL liposomes do not reflect a common structural arrangement, but distinct lipid environments that converge toward similarly restrictive conditions for dexamethasone accommodation. Thus, bilayer composition by itself was sufficient to generate local motional constraints comparable to, or exceeding, those found in solid or non-bilayer carriers. Drug loading was therefore defined less by formulation category than by the physical state of the lipid phase available for dexamethasone partitioning.

The methyl ester probes provided a complementary view of this behavior. In general, 5m exhibited lower τ_c values than 5d, indicating greater rotational freedom of the esterified probe in the more superficial hydrophobic region, consistent with weaker interfacial anchoring. Despite this difference in absolute mobility, the ranking among formulations was preserved, with HSPC-based liposomes remaining the most restricted systems and SPC-based liposomes the most mobile. The 16m data extended this trend to deeper regions of the lipid phase, showing again that the ordering associated with HSPC-rich bilayers was not confined to the interface.

Dexamethasone incorporation further altered the ESR response of the lipid phase. In the 5m spectra for which $2A_{||}$ could be extracted, all dexamethasone-loaded formulations showed higher values than their unloaded counterparts, consistent with increased local motional restriction after drug incorporation. Changes in τ_c values were also observed, although their magnitude and direction depended on both the probe and the formulation. These results indicate that dexamethasone perturbs lipid dynamics in a depth- and formulation-dependent manner, consistent with insertion into the hydrophobic region and modulation of local packing.[16,18]

In addition to the motional parameters τ_c and $2A_{||}$ the spectral-component profile of the convoluted ESR line shape also provided information on the internal organization of the nanocarriers. Experimental spectra containing two motional components indicate that the probes experience more than one local dynamic regime within the same carrier. Accordingly, the coexistence of S and W components reflects probe populations subject to different degrees of motional restriction, and therefore to distinct local fluidities, within the same lipid matrix. The W component is associated with probes in less constrained environments, whereas the S component corresponds to more restricted motion.[19,23,24] For 5d, the W component was clearly resolved only in SLN and NLC, indicating the coexistence of comparatively mobile regions with more ordered domains in these formulations. For 5m, the S component was evident in all spectra except those of SLN and NLC, suggesting that in these two systems the more immobilized population became less distinct. This spectral behavior indicates that that SLN and NLC presented a more heterogeneous and locally more dynamic lipid matrix than the other nanocarriers. The similar spectral response of SLN and NLC is also consistent with their similarly low EE and DL values, indicating that, under the present conditions, the partial reduction in matrix order expected for NLC was not sufficient to generate a fluidity profile distinguishable from that of SLN. Thus, although SLN are nominally regarded as more rigid and solid systems, their local dynamic behavior, as sensed by the spin probes, did not differ substantially from that observed for NLC. It should be noted, however, that ESR measurements report on local lipid mobility and heterogeneity, and do not resolve global crystallinity, polymorphism, or bulk lipid distribution.

Taken together, the ESR data identify local order and mobility as factors consistently correlated with dexamethasone accommodation. SPC-based liposomes combined high loading with the lowest motional restriction, whereas HSPC-based liposomes generated the most ordered local environments and the strongest limitation to incorporation. SLN, NLC, and LNP occupied an intermediate range of motional restriction, but remained unfavorable for efficient dexamethasone loading. These results establish the molecular basis for the release behavior described below.

Dexamethasone release

The release experiments were designed to determine how differences in local order, mobility, and carrier structure influence the kinetic profile of dexamethasone. In vitro release assays were therefore performed at 4 and 37 °C (Figure 3). The resulting profiles were strongly formulation-dependent, indicating that dexamethasone release was associated not only by its lipophilicity, but also by the local physicochemical environment in which it was accommodated.

At 37 °C, all formulations approached extensive release within the experimental time window, although with markedly different kinetics. HSPC-based liposomes, NLC, and SLN released nearly all incorporated dexamethasone within the first 2 h, whereas LNP and SPC-based liposomes showed slower release. Among the latter, SPC liposomes displayed the most sustained behavior, followed by SPC+CHOL and LNP. At 4 °C, the separation among formulations became more pronounced. HSPC+CHOL liposomes, NLC, and SLN retained a substantial fraction of dexamethasone even after 48 h, whereas SPC-based liposomes and LNP released a larger fraction under the same condition.

This temperature dependence was also evident from both the correlation analysis and the half-release times. In the correlation plot (Figure 4), HSPC-based liposomes, NLC, and SLN showed a larger deviation from the 1:1 relationship, indicating substantially higher release at 37 °C than at 4 °C, whereas SPC-

View Article Online
DOI: 10.1039/D6RM00126B

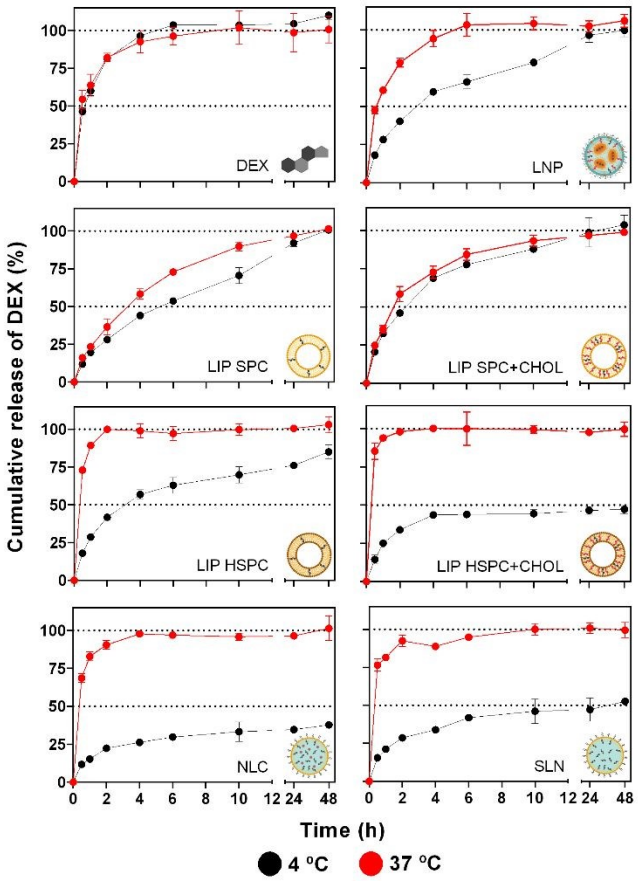

Figure 3 – In vitro cumulative release of Dexamethasone (DEX) from lipid nanoparticles in PBS (pH 7.4) at two temperatures. LNP = lipid nanoparticle; LIP = liposome; SPC = soy phosphatidylcholine; CHOL = cholesterol; HSPC = hydrogenated soy phosphatidylcholine; NLC = nanostructured lipid carrier; SLN = solid lipid nanoparticle. Values expressed as mean ± SD (n = 3).

based liposomes and LNP showed weaker divergence between the two temperatures. The same trend was reflected in the times required to reach 50% release (Table S2). At 37 °C, HSPC-based liposomes, SLN, and NLC reached 50% release within approximately 0.5 h, whereas LNP, SPC+CHOL liposomes, and SPC liposomes required approximately 1.0, 2.0, and 3.5 h, respectively. At 4 °C, this kinetic separation became much more pronounced: LNP, SPC+CHOL liposomes, and SPC liposomes required approximately 3.5, 3.0, and 6.0 h, respectively; HSPC liposomes reached 50% release at approximately 3.0 h; HSPC+CHOL liposomes and SLN required about 48 and 36 h, respectively; and NLC did not reach 50% release within the experimental time window. Since post-release particle size and morphology were not evaluated, the contribution of temperature-induced carrier destabilization or structural reorganization to the observed release profiles cannot be excluded.

This release behavior was consistent with the ESR results. HSPC-based liposomes combined the highest τ_c and $2A_{||}$ values with a pronounced temperature dependence in release. Although ESR indicated the most ordered and motion restricted lipid environment among the formulations, these systems released dexamethasone rapidly at 37 °C while retaining a substantially larger fraction at 4 °C, indicating that a highly ordered bilayer can limit dexamethasone accommodation at low temperature while remaining highly sensitive to temperature-dependent increases in permeability.[31]

SLN and NLC followed a related pattern. Both systems combined low EE and DL with strong temperature sensitivity in release, indicating that dexamethasone was accommodated in relatively restrictive lipid environments at low temperature but became more diffusible as temperature increased. Despite their compositional differences, their release profiles remained broadly similar, indicating that the modification introduced in NLC, the partial replacement of stearic acid by oleic acid, was insufficient under the present conditions to generate local lipid dynamics or release pattern distinguishable from that of SLN, as assessed by the parameters evaluated in this study.

SPC-based liposomes showed a distinct behavior. These formulations combined the highest EE and DL values with the lowest motional restriction and displayed the slowest release kinetics, particularly at 4 °C. This result indicates that high

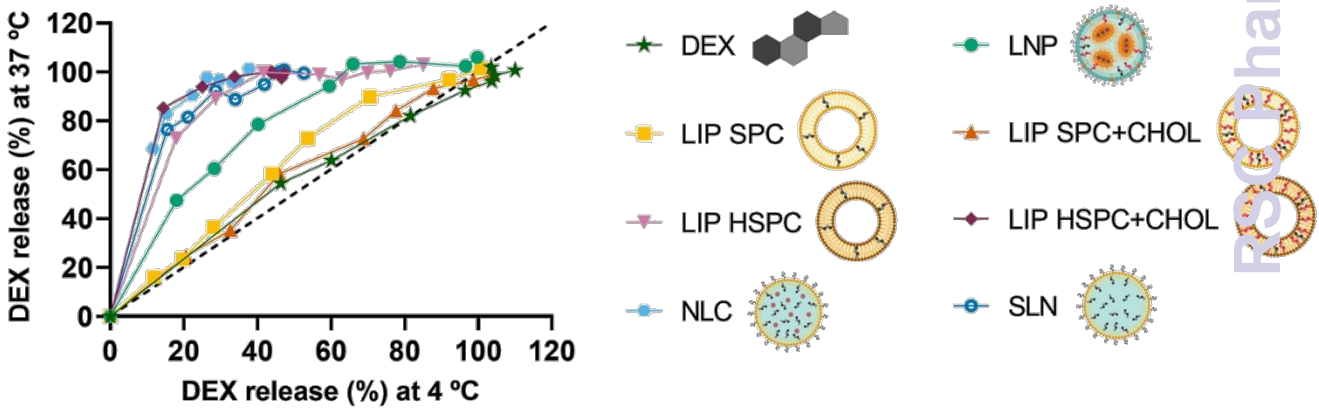

Figure 4 - Correlation between Dexamethasone release at 37 °C and 4 °C across different lipid-based nanocarriers. Black dashed line represents the 1:1 correlation line.

View Article Online
DOI: 10.1039/D6PM00126B

loading capacity and slower release can coexist when the drug is accommodated in a fluid bilayer that remains permissive to partitioning without undergoing abrupt permeability changes over the studied range. Cholesterol shifted this behavior toward slightly greater order and faster release. This formulation-dependent release profile is consistent with previous reports showing that dexamethasone retention varies markedly with liposomal organization and structural stability.[32]

LNP displayed different release kinetics from both phospholipid bilayers and fatty-acid-based matrices. Although these particles exhibited low EE and DL, their release was comparatively moderate and less temperature-dependent than that of HSPC-based liposomes, SLN, or NLC. This result indicates that the limited loading capacity of LNP cannot be attributed solely to local motional restriction but is also consistent with reduced accessibility of drug-compatible regions within a structurally complex lipid phase.

Overall, formulation-dependent differences in composition were directly reflected in dexamethasone incorporation, lipid mobility, and release profile. SPC-based liposomes combined high loading, low motional restriction, and comparatively sustained release, whereas HSPC-based liposomes generated the most ordered lipid environments and the strongest temperature dependence in release. SLN, NLC, and LNP, despite their distinct structural features, converged toward comparatively unfavorable conditions for dexamethasone accommodation. Within this dataset, the strongest thermal effect was observed for HSPC+CHOL liposomes, SLN, and NLC, whereas SPC-based liposomes and LNP showed comparatively weaker temperature dependence. These results indicate that dexamethasone behavior across these systems is correlated with the way each formulation defined the physical state of the lipid phase available for drug partitioning and diffusion.

Release kinetic analysis

To further investigate the mechanisms underlying formulation-dependent release behavior, the experimental release profiles were fitted to zero-order, first-order, Higuchi, Korsmeyer–Peppas, Weibull, Hixson–Crowell, and Baker–Lonsdale models (Tables S3 and S4). Considerable differences in model performance were observed among formulations and temperatures, indicating that dexamethasone release could not be universally described by a single classical kinetic mechanism.

Among all evaluated models, the Weibull equation consistently provided the best fit for most formulations at both temperatures. R^2 values frequently exceeded 0.90 and approached unity for SPC-based liposomes and LNP, whereas the alternative models generally showed lower coefficients of determination. The superior performance of the Weibull model suggests that dexamethasone release is governed by multiple concurrent processes rather than by a single rate-limiting mechanism. Such behavior is consistent with heterogeneous lipid environments in which diffusion, partitioning, and temperature-dependent structural rearrangements may simultaneously contribute to drug release.[33,34]

The Hixson–Crowell model generally showed poorer performance than the Weibull model, particularly for HSPC-based liposomes, SLN, and NLC. Because this model assumes that release is primarily controlled by changes in particle surface area and geometry during dissolution,[35] its limited applicability suggests that erosion- or dissolution-controlled mechanisms are not the dominant drivers of dexamethasone release in these systems. This interpretation is consistent with the lipidic nature of the carriers.

Similarly, the Baker–Lonsdale model, which describes diffusion-controlled release from homogeneous spherical matrices,[36] provided only moderate fits for a subset of formulations and performed particularly poorly for several systems at 37 °C. Notably, the quality of fit decreased markedly for HSPC-containing liposomes, NLC, and SLN at the higher temperature. If diffusion from a homogeneous spherical matrix were the dominant mechanism, the model would be expected to retain predictive capacity across temperatures. Instead, the observed loss of fit indicates that temperature-dependent changes in lipid organization and permeability contribute substantially to the release process.[37–39]

The kinetic analysis further supports the interpretation derived from ESR measurements. Formulations characterized by highly ordered lipid environments, such as HSPC-based liposomes, exhibited the strongest temperature dependence and the poorest agreement with classical diffusion- and erosion-based models. In contrast, SPC-based liposomes, which displayed the lowest motional restriction and the highest dexamethasone loading, showed excellent agreement with the Weibull model while maintaining comparatively slow-release kinetics. These observations indicate that release behavior depends not only on diffusional transport but also on the dynamic properties of the lipid phase in which dexamethasone is accommodated.[38,39]

Although the Weibull model most frequently yielded the highest R^2 values in the present study, recent comparative analyses have shown that both Korsmeyer–Peppas and Weibull models can adequately describe drug release from lipid-based nanoparticles.[40] The Korsmeyer–Peppas model could only be reliably applied to a limited number of formulations because several systems exceeded 60% release within the early sampling intervals, resulting in an insufficient number of data points within the range required by the model. Consequently, the relatively rapid release observed for some formulations may have restricted the applicability of the Korsmeyer–Peppas approach and favored more flexible empirical descriptions such as Weibull. For the formulations in which the model was applicable, the release exponents ranged from 0.23 to 0.60, suggesting distinct transport behaviors depending on lipid composition. Therefore, these values should be regarded as complementary indicators rather than definitive descriptors of the release mechanism.

Overall, the kinetic modeling results reinforce the central conclusion emerging from both the release and ESR datasets: dexamethasone release is more strongly associated with lipid-phase organization and membrane dynamics than with nanocarrier classification alone. The inability of diffusion- or erosion-based models to consistently describe all formulations, together with the superior performance of the Weibull equation, indicates that release is governed by the combined effects of molecular diffusion, lipid packing, and temperature-dependent structural rearrangements within the carrier matrix.[33,37–39]

It should be noted that the formulations compared here differ not only in lipid phase organization, but also in interfacial charge, excipient composition, and supramolecular architecture, variables that are intrinsic to each carrier class and cannot be independently eliminated in a cross-platform design. The observed associations between ESR-derived lipid dynamics and dexamethasone encapsulation and release are therefore interpreted as strong correlations rather than evidence of a single causal determinant.

Experimental

Chemicals

Dexamethasone (DEX), cholesterol (CHOL), 1,2-dioleoyl-3-trimethylammonium-propane (DOTAP), 1,2-distearoyl-sn-glycero-3-phosphocholine (DSPC), 1,2-distearoyl-sn-glycero-3-phosphoethanolamine-poly(ethylene glycol)2000 (DSPE-PEG2000), sodium taurodeoxycholate (TDC), 5-doxyl stearic acid methyl ester (5m), 16-doxyl stearic acid methyl ester (16m), 5-doxyl stearic acid (5d), 16-doxyl stearic acid (16d), stearic acid, and oleic acid were purchased from Sigma-Aldrich (Merck KGaA, Germany). Highly unsaturated soybean phosphatidylcholine (SPC, LIPOID S100) and hydrogenated soybean phosphatidylcholine (HSPC, LIPOID P75-3) were purchased from Lipoid GmbH (Germany). All other solvents and reagents were of analytical grade or higher.

Analytical assays

High-performance liquid chromatography (HPLC) analyses were performed according to the Brazilian Pharmacopeia,[41] with modifications. dexamethasone quantification was carried out using an Agilent 1260 Infinity HPLC system (Agilent, USA) equipped with a Zorbax SB-C18 column (150 × 4.6 mm, 5 µm), maintained at 40 °C. The mobile phase consisted of methanol:water (70:30, v/v) under isocratic elution at a flow rate of 1.0 mL/min. The injection volume was 20 µL, and detection was performed at 240 nm. The retention time of dexamethasone was 3.25 min.

Preparation of lipid nanocarriers

Preparation of LNP

LNP were prepared by the ethanol injection method as previously described.[42] Briefly, all formulation components were dissolved in ethanol (99.5%) to form the organic phase, using a molar ratio of DOTAP:DSPC:CHOL:DSPE-PEG2000:PAM:DEX of 50:10:38.5:1.5:7:1.5. The organic phase was mixed with sodium citrate buffer (5 mM, pH 3.0) at a 1:3 ratio, followed by addition of PBS (pH 7.4) at a 1:2 ratio. The resulting dispersion was dialyzed against PBS (pH 7.4) to remove ethanol.

Preparation of liposomes

In this study, four dexamethasone-loaded liposomal formulations were prepared using either soy phosphatidylcholine (SPC) or hydrogenated soy phosphatidylcholine (HSPC) as the main structural lipid, in the absence or presence of cholesterol (CHOL). The lipid compositions were selected based on previous liposomal formulations reported in the literature and on the well-established effects of phospholipid saturation and cholesterol on bilayer organization and membrane order.[18,19,43] The compositions were defined relative to the phospholipid molar amount as follows: SPC:DEX (100:5), SPC:CHOL:DEX (100:30:5), HSPC:DEX (100:5), and HSPC:CHOL:DEX (100:30:5), all expressed as molar ratios.

The liposomes were prepared at a total phospholipid concentration of 40 mM. Lipids and dexamethasone were dissolved in chloroform, and a thin lipid film was formed by rotary evaporation under reduced pressure (IKA RV 10). The films were then hydrated with ultrapure water to obtain multilamellar vesicle suspensions. Unilamellar liposomes were produced by extrusion through polycarbonate membranes with 0.1 µm pores.

Preparation of SLN and NLC

SLN and NLC were prepared by the microemulsion method according to Silva et al,[44] with modifications. The SLN microemulsion was composed of stearic acid (160 mg), SPC (80 mg), sodium taurodeoxycholate (120 mg), and dexamethasone (12 mg). The NLC microemulsion was composed of stearic acid (120 mg), oleic acid (40 mg), SPC (80 mg), sodium taurodeoxycholate (120 mg), and dexamethasone (12 mg).

Briefly, all components were dissolved in 1 mL of ethanol and 1 mL of ultrapure water and stirred magnetically at 80 °C until transparent emulsions were obtained. Subsequently, 20 mL of cold water (2-4 °C) was added under vigorous stirring (24,000 rpm for 10 min; IKA T25 Ultra-Turrax, Königswinter, Germany). Excess sodium taurodeoxycholate and dexamethasone were removed by a 10-fold dilution in cold water followed by concentration using Amicon® ultracentrifugal filters (100,000 MWCO) at 1,000 rcf.

Lipid nanocarriers characterization

Mean hydrodynamic diameter and polydispersity index (PdI) were measured by dynamic light scattering, and zeta potential was determined from electrophoretic mobility using a Zetasizer Nano ZS90 (Malvern Instruments Ltd., Worcestershire, UK).

View Article Online
DOI: 10.1039/D6PM00126B

Nanoparticle concentration was determined by nanoparticle tracking analysis (NTA) using a NanoSight NS500 (NanoSight, Amesbury, UK) equipped with a 532 nm laser and an EMCCD 215S camera (Beckman Coulter, Marseille, France).

For encapsulation efficiency (EE) and drug loading (DL) analyses, a 20 µL aliquot of each formulation was diluted in 980 µL of methanol, vortexed for 10 s, and filtered through a 0.45 µm PVDF membrane prior to HPLC quantification.

Encapsulation efficiency was calculated as:

$$EE(\%) = \frac{m_{enc}}{m_0} x100$$

where m_{enc} is the mass of encapsulated drug and m_0 is the initial mass of drug added.

Drug loading was calculated as:

$$DL\left(\frac{\mu M}{mM}\right) = \frac{n_{enc}}{C_{lip}}$$

where n_{enc} is the amount of encapsulated drug (µM) and C_{lip} is the total lipid concentration (mM).

Electron spin resonance measurements

Electron spin resonance (ESR) measurements were conducted with a Bruker EMXplus spectrometer equipped with a PremiumX microwave bridge operating in the X-band (9.4 GHz) and a high-sensitivity resonant cavity. All measurements were performed at room temperature (24-26 °C). Instrumental parameters included: microwave power, 2.0 mW; modulation frequency, 100 kHz; amplitude of modulation, 1.0 G; magnetic field scan, 100 G; scan time, 168 s, and detection time constant, 41 ms. Lipid dynamics were evaluated after addition of the nitroxide probes. A mixture of 60 µL of each formulation and 0.5 µL of the desired spin label (5 mg/mL) was placed in a flame-sealed glass capillary, which was then inserted into the equipment's cavity.

ESR spectra analysis

The best-fitting of ESR spectra were performed using the NLLS software developed by Freed et al.[45] The rotational diffusion rate, Rbar, obtained from NLLS was converted to rotational correlation time, τ_c, through the relation (Brownian rotational diffusion):

$$\tau_c = \frac{1}{6R_{bar}}$$

The experimental spectra were fitted using a molecular model of 1 or 2 spectral components. Similarly to other studies,[19,24,46] the magnetic parameters were determined based on a global analysis of the set of obtained spectra, and all spectra were simulated using the same input parameters for the g and A magnetic tensors. For those spectra of highly anisotropic lineshape, the maximum hyperfine splitting parameter ($2A_{||}$) values, obtained directly from the experimental line, were also used as a measure of membrane rigidity, as previously described.[29,43]

Dexamethasone release assay

In vitro cumulative release of dexamethasone was evaluated using dialysis bags with a molecular weight cutoff of 12-14 kDa. An aliquot of each formulation was placed inside the dialysis bag and incubated in 200 mL of phosphate-buffered saline (PBS, pH 7.4) under magnetic stirring (200 rpm) at either 4 or 37 °C. At predetermined time points (0.5, 1, 2, 4, 6, 10, 24, and 48 h), 1 mL of release medium was collected and replaced with 1 mL of fresh PBS.

The collected samples were lyophilized, and the residue was dissolved in 250 µL of methanol, filtered through a 0.45 µm PVDF membrane, and quantified by HPLC. For comparison, free dexamethasone was prepared by dissolving 500 µg of dexamethasone in 25 µL of ethanol, followed by addition of 975 µL of water, and the resulting solution was placed in dialysis cassettes under the same conditions.

Cumulative dexamethasone release was calculated as:

$$Release(\%) = \frac{m_{acc}}{m_0} x100$$

where m_{acc} is the mass of dexamethasone in the acceptor medium and m_0 is the initial mass of drug added.

Drug release kinetic analysis

The cumulative dexamethasone release profiles obtained at 4 and 37 °C were fitted to zero-order, first-order,[34] Higuchi,[47] Korsmeyer–Peppas,[48] Weibull[33], Hixson–Crowell[35], and Baker–Lonsdale[36] kinetic models to investigate the mechanisms associated with drug release from the different lipid nanocarriers. The mathematical expressions employed were:

Zero order:

$$Q_t = Q_0 + k_0 t$$

First order:

$$ln(100 - Q_t) = ln(100) - k_1 t$$

Higuchi:

$$Q_t = k_H t^{1/2}$$

Korsmeyer–Peppas:

$$\frac{M_t}{M_\infty} = kt^n$$

Weibull:

$$F(t) = 100\left(1 - e^{-\left(\frac{t}{a}\right)^b}\right)$$

Hixson–Crowell:

$$(100 - Q_t)^{\frac{1}{3}} = 100^{\frac{1}{3}} - k_{(HC)t}$$

Baker–Lonsdale:

$$\frac{3}{2}\left[1 - (1 - F)^{\frac{2}{3}}\right] - \frac{M_t}{M_\infty} = k_{BL} t$$

Where:
Q_t is the cumulative percentage of dexamethasone released at time t
Q_0 is the initial amount released
$\frac{M_t}{M_\infty}$ is the fraction of drug released at time t
F is the fraction of dexamethasone released $\frac{\mathrm{Q_t}}{100}$
k is the kinetic constant of the respective model
n is the release exponent associated with the release mechanism
a is the Weibull scale parameter
b is the Weibull shape parameter
$k_{BL}t$ is the Baker–Lonsdale release constant.

Linear regression analyses were performed using GraphPad Prism version 9 (GraphPad Software, USA) for the zero-order, first-order, Higuchi, Korsmeyer–Peppas, Hixson–Crowell, and Baker–Lonsdale models, whereas the Weibull model was fitted by nonlinear regression. The goodness of fit was assessed by the coefficient of determination (R^2).

For Korsmeyer–Peppas analysis, only release values corresponding to less than 60% cumulative release were considered, according to the original model assumptions.[48] When an insufficient number of experimental points was available within this range, reliable estimation of model parameters was not possible and the model was not applied. For first-order fitting, points corresponding to complete release (100%) were excluded because logarithmic transformation becomes mathematically undefined under these conditions.[34] The kinetic model presenting the highest R^2 value was considered to provide the best mathematical description of the release profile, and its interpretation was further evaluated in the context of the structural and biophysical characteristics of each nanocarrier.

Conclusions

This study demonstrates that dexamethasone behavior across lipid nanocarriers is consistently associated with the physicochemical state of the lipid phase established in each formulation. Among the systems investigated, SPC-based liposomes combined the highest encapsulation efficiency and drug loading with the lowest motional restriction detected by ESR and the slowest release kinetics, indicating that a less ordered bilayer favors both dexamethasone accommodation and sustained release. In contrast, HSPC-based liposomes exhibited the highest τc and $2A_{||}$ values, showing that saturated phosphatidylcholine bilayers generated the most motionally restricted local environments in the dataset, even exceeding those observed for SLN and LNP. Despite this high degree of order, HSPC-based liposomes displayed the strongest temperature dependence in release, indicating that highly ordered membranes can strongly limit drug accommodation while remaining sensitive to temperature-induced changes in permeability. Although differing in composition and supramolecular architecture, SLN, NLC, and LNP converged toward comparatively unfavorable conditions for dexamethasone accommodation. In particular, SLN and NLC exhibited indistinguishable local lipid dynamics under the present conditions, indicating that the incorporation of oleic acid into NLC was insufficient to substantially modify the physicochemical environment available for drug partitioning.

Overall, the results indicate that drug behavior is more closely related to lipid-phase organization and membrane dynamics than to nanocarrier classification alone. The correlations observed between ESR-derived mobility parameters, encapsulation efficiency, and release kinetics support the use of these parameters as informative descriptors for interpreting formulation-dependent differences in drug accommodation and diffusion. Dexamethasone was selected not only because of its favorable physicochemical properties, but also because it represents one of the most extensively investigated lipophilic corticosteroids in nanomedicine. Previous studies have employed dexamethasone in liposomes, SLN, NLC, LNP, and polymeric nanoparticles for a broad range of therapeutic applications (Table S5). Therefore, the relationships between lipid organization, drug partitioning, and release identified here are expected to be relevant, with appropriate optimization, to structurally related corticosteroids and other membrane-partitioning small molecules with comparable size and lipophilicity. Nevertheless, extrapolation to other hydrophobic drugs should be made cautiously, since drug-specific factors, including molecular geometry, hydrogen-bonding capacity, and membrane affinity, may influence their interactions with lipid phases.

Abbreviations list

CHOL	Cholesterol
DEX	Dexamethasone
DL	Drug loading
DOTAP	1,2-dioleoyl-3-trimethylammonium-propane
DSPC	Distearoylphosphatidylcholine
DSPE-PEG2000	1,2-distearoyl-sn-glycero-3-phosphoethanolamine-poly(ethylene glycol)2000
EE	Encapsulation efficiency
ESR	Electron spin resonance
HPLC	High-performance liquid chromatography
HSPC	Hydrogenated soybean phosphatidylcholine
LNP	Lipid nanoparticle
NLC	Nanostructured lipid carrier
PAM	polyanionic molecule
PdI	Polydispersity index
SLN	Solid lipid nanoparticle
SPC	Soy phosphatidylcholine
TDC	Sodium taurodeoxycholate

5d	5-doxyl stearic acid
5m	5-doxyl stearic acid methyl ester
16d	16-doxyl stearic acid
16m	16-doxyl stearic acid methyl ester

Author contributions

J.P., L.R.S., and B.B.F. were responsible for the acquisition of experimental data. All authors contributed to the writing and revision of the manuscript. S.A.M. and E.M.L. conceived and designed the experimental protocols, secured funding, and provided supervision throughout the development of the study.

Conflicts of interest

There are no conflicts to declare.

Data availability

The data supporting the findings of this study are available from the corresponding author upon reasonable request. All relevant data generated or analyzed during this study are included in this article and its Supplementary Information. Additional raw datasets, including physicochemical characterization, electron spin resonance (ESR) analyses, and in vitro release profiles, are available to support reproducibility and further analysis.

Acknowledgements

This study was financed in part by the Coordenação de Aperfeiçoamento de Pessoal de Nível Superior – Brasil (CAPES) – Finance Code 001. The authors acknowledge financial support from the Conselho Nacional de Desenvolvimento Científico e Tecnológico (CNPq), and the Fundação de Amparo à Pesquisa do Estado de Goiás (FAPEG). This work was also supported by the Instituto Nacional de Ciência e Tecnologia em Nanotecnologia Farmacêutica (INCT NanoFarma). The authors thank Professor Nicolas Bertrand (Université Laval, Canada) for valuable discussions and insightful suggestions regarding figure design and visual presentation of the data.

AI Use Statement

During the preparation of this manuscript, the authors used ChatGPT by OpenAI and Claude by Anthropic exclusively for language editing, grammar refinement, and improvement of textual clarity. No AI tools were used for data generation, data analysis, interpretation of results, or preparation of scientific conclusions. All content was critically reviewed, verified, and approved by the authors, who take full responsibility for the final manuscript.

References

1 M. Mehta, T. A. Bui, X. Yang, Y. Aksoy, E. M. Goldys and W. Deng, Lipid-Based Nanoparticles for Drug/Gene Delivery: An Overview of the Production Techniques and Difficulties Encountered in Their Industrial Development, *ACS Mater. Au*, 2023, **3**, 600–619.

2 J. Menge, C. Yang, D. A. Weitz and K. Jahnke, Engineering the biophysical properties of lipid nanostructures for drug delivery, *Commun. Mater.*, 2026, **7**, 25.

3 V. P. Torchilin, Recent advances with liposomes as pharmaceutical carriers, *Nat. Rev. Drug Discov.*, 2005, **4**, 145–160.

4 M. J. Mitchell, M. M. Billingsley, R. M. Haley, M. E. Wechsler, N. A. Peppas and R. Langer, Engineering precision nanoparticles for drug delivery, *Nat. Rev. Drug Discov.*, 2021, **20**, 101–124.

5 J. Akbari, M. Saeedi, F. Ahmadi, S. M. H. Hashemi, A. Babaei, S. Yaddollahi, S. S. Rostamkalaei, K. Asare-Addo and A. Nokhodchi, Solid lipid nanoparticles and nanostructured lipid carriers: a review of the methods of manufacture and routes of administration, *Pharm. Dev. Technol.*, 2022, **27**, 525–544.

6 A. Gordillo-Galeano and C. E. Mora-Huertas, Solid lipid nanoparticles and nanostructured lipid carriers: A review emphasizing on particle structure and drug release, *Eur. J. Pharm. Biopharm.*, 2018, **133**, 285–308.

7 C. A. Brimacombe, J. A. Kulkarni, M. H. Y. Cheng, K. An, D. Witzigmann and P. R. Cullis, Rational design of lipid nanoparticles for enabling gene therapies, *Mol. Ther. Methods Clin. Dev.*, 2025, **33**, 101518.

8 X. Hou, T. Zaks, R. Langer and Y. Dong, Lipid nanoparticles for mRNA delivery, *Nat. Rev. Mater.*, 2021, **6**, 1078–1094.

9 J. Fralliciardi, J. Melcr, P. Siginou, S. J. Marrink and B. Poolman, Membrane thickness, lipid phase and sterol type are determining factors in the permeability of membranes to small solutes, *Nat. Commun.*, 2022, **13**, 1605.

10 K. Atkovska, J. Klingler, J. Oberwinkler, S. Keller and J. S. Hub, Rationalizing Steroid Interactions with Lipid Membranes: Conformations, Partitioning, and Kinetics, *ACS Cent. Sci.*, 2018, **4**, 1155–1165.

11 S. L. Regen, Cholesterol's Condensing Effect: Unpacking a Century-Old Mystery, *JACS Au*, 2022, **2**, 84–91.

12 T.-H. Lee, P. Charchar, F. Separovic, G. E. Reid, I. Yarovsky and M.-I. Aguilar, The intricate link between membrane lipid structure and composition

View Article Online DOI: 10.1039/D6PM00126B

View Article Online
DOI: 10.1039/D6PM00126B

and membrane structural properties in bacterial membranes, *Chem. Sci.*, 2024, **15**, 3408–3427.
13 PubChem, Dexamethasone, https://pubchem.ncbi.nlm.nih.gov/compound/5743, (accessed 19 May 2026).
14 DrugBank Online, Dexamethasone, https://go.drugbank.com/drugs/DB01234, (accessed 19 May 2026).
15 J. Crowley, M. Withana and E. Deplazes, The interaction of steroids with phospholipid bilayers and membranes, *Biophys. Rev.*, 2022, **14**, 163–179.
16 C. I. Cámara, M. A. Crosio, A. V. Juarez and N. Wilke, Dexamethasone and Dexamethasone Phosphate: Effect on DMPC Membrane Models, *Pharmaceutics*, 2023, **15**, 844.
17 C. I. Camara, L. Bertocchi, C. Ricci, R. Bassi, A. Bianchera, L. Cantu', R. Bettini and E. Del Favero, Hyaluronic Acid—Dexamethasone Nanoparticles for Local Adjunct Therapy of Lung Inflammation, *Int. J. Mol. Sci.*, 2021, **22**, 10480.
18 V.-A. Tsotas, S. Mourtas and S. G. Antimisiaris, Dexamethasone Incorporating Liposomes: Effect of Lipid Composition on Drug Trapping Efficiency and Vesicle Stability, *Drug Deliv.*, 2007, **14**, 441–445.
19 K. Bohne Japiassu, F. Fay, A. Marengo, S. A. Mendanha, C. Cailleau, Y. Louaguenouni, Q. Wang, S. Denis, N. Tsapis, T. Leite Nascimento, E. Martins Lima and E. Fattal, Hyaluronic acid-conjugated liposomes loaded with dexamethasone: A promising approach for the treatment of inflammatory diseases, *Int. J. Pharm.*, 2023, **639**, 122946.
20 L. Xu, X. Wang, Y. Liu, G. Yang, R. J. Falconer and C.-X. Zhao, Lipid Nanoparticles for Drug Delivery, *Adv. NanoBiomed Res.*, 2022, **2**, 2100109.
21 A. S. Alfutaimani, N. K. Alharbi, A. S. Alahmari, A. A. Alqabbani and A. M. Aldayel, Exploring the landscape of Lipid Nanoparticles (LNPs): A comprehensive review of LNPs types and biological sources of lipids, *Int. J. Pharm. X*, 2024, **8**, 100305.
22 L. Gomes Souza, A. Antonio Sousa-Junior, B. Alves Santana Cintra, J. L. Vieira Dos Anjos, T. Leite Nascimento, L. Palmerston Mendes, M. De Souza Vieira, R. Do Nascimento Ducas, M. Campos Valadares, S. Antônio Mendanha and E. Martins Lima, Pre-clinical safety of topically administered sunitinib-loaded lipid and polymeric nanocarriers targeting corneal neovascularization, *Int. J. Pharm.*, 2023, **635**, 122682.
23 S. A. Mendanha, J. L. V. Dos Anjos, L. Maione-Silva, H. C. B. Silva, E. M. Lima and A. Alonso, An EPR spin probe study of the interactions between PC liposomes and stratum corneum membranes, *Int. J. Pharm.*, 2018, **545**, 93–100.
24 S. A. Mendanha and A. Alonso, Effects of terpenes on fluidity and lipid extraction in phospholipid membranes, *Biophys. Chem.*, 2015, **198**, 45–54.
25 R. J. Alsop, A. Khondker, J. S. Hub and M. C. Rheinstädter, The Lipid Bilayer Provides a Site for Cortisone Crystallization at High Cortisone Concentrations, *Sci. Rep.*, 2016, **6**, 22425.
26 M. Ur-Rehman, F. Reynaud, S. Lepetre, S. Abreu, P. Chaminade, E. Fattal and N. Tsapis, *J. Controlled Release*, 2023, 360, 293–303.
27 Y. Zong, H. Zhong, Y. Wang, Y. Lin, L. Zhao, X. Wang, J. Cai, H. Lin, Y. Xiao, T. Wei, S. Guo and Q. Cheng, Safe and Highly Efficient Lipid-Pro-Dexamethasone Nanoparticles for mRNA Delivery and Base Editing, *J. Am. Chem. Soc.*, 2026, **148**, 10225–10240.
28 K. Ondriaš, Use of electron spin resonance spectroscopy of spin labels for studying drug-induced membrane perturbation, *J. Pharm. Biomed. Anal.*, 1989, **7**, 649–675.
29 L. Alonso, S. A. Mendanha, M. L. Dorta and A. Alonso, Analysis of the Interactions of Amphotericin B with the *Leishmania* Plasma Membrane Using EPR Spectroscopy, *J. Phys. Chem. B*, 2020, **124**, 10157–10165.
30 S. P. N. Bukke, C. Venkatesh, S. Bandenahalli Rajanna, T. S. Saraswathi, P. K. Kusuma, N. Goruntla, N. Balasuramanyam and S. Munishamireddy, Solid lipid nanocarriers for drug delivery: design innovations and characterization strategies—a comprehensive review, *Discov. Appl. Sci.*, 2024, **6**, 279.
31 A. Blicher, K. Wodzinska, M. Fidorra, M. Winterhalter and T. Heimburg, The Temperature Dependence of Lipid Membrane Permeability, its Quantized Nature, and the Influence of Anesthetics, *Biophys. J.*, 2009, **96**, 4581–4591.
32 P. Kallinteri, S. Antimisiaris, D. Karnabatidis, C. Kalogeropoulou, I. Tsota and D. Siablis, *BIOMATERIALS*, 2002, 23, 4819–4826.
33 V. Papadopoulou, K. Kosmidis, M. Vlachou and P. Macheras, On the use of the Weibull function for the discernment of drug release mechanisms, *Int. J. Pharm.*, 2006, **309**, 44–50.
34 P. Costa and J. M. Sousa Lobo, Modeling and comparison of dissolution profiles, *Eur. J. Pharm. Sci.*, 2001, **13**, 123–133.
35 A. W. Hixson and J. H. Crowell, Dependence of Reaction Velocity upon surface and Agitation, *Ind. Eng. Chem.*, 1931, **23**, 923–931.

36 S. Dash, P. N. Murthy, L. Nath and P. Chowdhury, KINETIC MODELING ON DRUG RELEASE FROM CONTROLLED DRUG DELIVERY SYSTEMS.

37 J. Siepmann and N. A. Peppas, Higuchi equation: Derivation, applications, use and misuse, *Int. J. Pharm.*, 2011, **418**, 6–12.

38 W. Mehnert and K. Mäder, Solid lipid nanoparticles: Production, characterization and applications, *Adv. Drug Deliv. Rev.*, 2001, **47**, 165–196.

39 R. H. Müller, M. Radtke and S. A. Wissing, Solid lipid nanoparticles (SLN) and nanostructured lipid carriers (NLC) in cosmetic and dermatological preparations, *Adv. Drug Deliv. Rev.*, 2002, **54**, S131–S155.

40 P. Porbaha, R. Ansari, M. R. Kiafar, R. Bashiry, M. M. Khazaei, A. Dadbakhsh and A. Azadi, A Comparative Mathematical Analysis of Drug Release from Lipid-Based Nanoparticles, *AAPS PharmSciTech*, 2024, **25**, 208.

41 Agência Nacional de Vigilância Sanitária (ANVISA), Ed., in *Insumos Farmacêuticos e Especialidades*, Brasília, 6th edn., 2019, vol. II – Monografias.

42 X. Wang, S. Liu, Y. Sun, X. Yu, S. M. Lee, Q. Cheng, T. Wei, J. Gong, J. Robinson, D. Zhang, X. Lian, P. Basak and D. J. Siegwart, Preparation of selective organ-targeting (SORT) lipid nanoparticles (LNPs) using multiple technical methods for tissue-specific mRNA delivery, *Nat. Protoc.*, 2023, **18**, 265–291.

43 A. C. M. Barros, J. Pires, K. Mendanha, L. R. De Sousa, B. B. Fontanezi, G. Colherinhas, A. F. M. Botelho, S. A. Mendanha and E. M. Lima, Cholesterol-Driven Optimization of Liposomal Systems for Ivermectin Capture: Insights from Experimental and Molecular Dynamics Studies, *ACS Appl. Mater. Interfaces*, 2026, **18**, 10832–10841.

44 L. A. D. Silva, L. M. Andrade, F. A. P. de Sá, R. N. Marreto, E. M. Lima, T. Gratieri and S. F. Taveira, Clobetasol-loaded nanostructured lipid carriers for epidermal targeting, *J. Pharm. Pharmacol.*, 2016, **68**, 742–750.

45 D. E. Budil, S. Lee, S. Saxena and J. H. Freed, Nonlinear-Least-Squares Analysis of Slow-Motion EPR Spectra in One and Two Dimensions Using a Modified Levenberg–Marquardt Algorithm, *J. Magn. Reson. A*, 1996, **120**, 155–189.

46 S. A. Mendanha, C. A. Marquezin, A. S. Ito and A. Alonso, Effects of nerolidol and limonene on stratum corneum membranes: A probe EPR and fluorescence spectroscopy study, *Int. J. Pharm.*, 2017, **532**, 547–554.

47 T. Higuchi, Mechanism of sustained-action medication. Theoretical analysis of rate of release of solid drugs dispersed in solid matrices, *J. Pharm. Sci.*, 1963, **52**, 1145–1149.

48 R. W. Korsmeyer, R. Gurny, E. Doelker, P. Buri and N. A. Peppas, Mechanisms of solute release from porous hydrophilic polymers, *Int. J. Pharm.*, 1983, **15**, 25–35.

View Article Online
DOI: 10.1039/D6PM00126B

View Article Online
DOI: 10.1039/D6PM00126B

Lipid Phase Organization Controls Drug Partitioning and Release Across Lipid Nanocarriers

Jader Pires,[#a,b] Lucas R. de Souza,[#a,c] Bianca B. Fontanezi,[a,b] Sebastião A. Mendanha[a,c] and Eliana M. Lima [*a,b]
[a.] FarmaTec - Laboratory for RD&I in Pharmaceutical Nanotechnology and Drug Delivery Systems, Samambaia Technology Park, UFG, Goiânia - GO – Brazil
[b.] School of Pharmacy, Federal University of Goiás, Goiania, 74690-631, Brazil
[c.] Institute of Physics, Federal University of Goias, Goiania, 74605-220 Goias, Brazil
[#] J.P. and L.R.S contributed equally to this work.
* Corresponding author: emlima@ufg.br

Data availability statement

The data supporting the findings of this study are available from the corresponding author upon reasonable request. All relevant data generated or analyzed during this study are included in this article and its Supplementary Information. Additional raw datasets, including physicochemical characterization, electron spin resonance (ESR) analyses, and in vitro release profiles, are available to support reproducibility and further analysis.